Oetting, W. S., Ho, T. W. C., Greenan, J. R., & Walker, A. M. (1989) *Mol. Cell. Endocrinol. 61*, 189-199.
Pigiet, V. P., & Schuster, B. J. (1986) *Proc. Natl. Acad. Sci. U.S.A. 83*, 7643-7647.
Powers, C. A. (1986) *Mol. Cell. Endocrinol. 46*, 163-174.
Powers, C. A. (1987) *Endocrinology 120*, 429-431.
Powers, C. A., & Hatala, M. A. (1986) *Neuroendocrinology 44*, 462-469.
Powers, C. A., & Hatala, M. A. (1990) *Endocrinology 127*, 1916-1927.
Powers, C. A., & Nasjletti, A. (1984) *Endocrinology 114*, 1841-1844.
Rozell, B., Hansson, H.-A., Luthman, M., & Holmgren, A. (1985) *Eur. J. Cell Biol. 38*, 79-86.
Sagar, S. M., Millard, W. J., Martin, J. B., & Murchison, S. C. (1985) *Endocrinology 117*, 591-600.
Scammell, J. G., Burrage, T. G., Eisenfeld, A. J., & Dannies, P. S. (1985) *Endocrinology 116*, 2347-2354.
Shah, G. N., & Hymer, W. C. (1989) *Mol. Cell. Endocrinol. 61*, 97-107.
Sinha, Y. N., & Jacobsen, B. B. (1988) *Endocrinology 123*, 1364-1370.
Vio, C. P., Roa, J. P., Silva, R., & Powers, C. A. (1990) *Neuroendocrinology 51*, 10-14.

Secondary Structure Analysis of the Scrapie-Associated Protein PrP 27-30 in Water by Infrared Spectroscopy†

Byron W. Caughey,*,‡ Aichun Dong,§ Kolari S. Bhat,‡ Darwin Ernst,‡ Stanley F. Hayes,‡ and Winslow S. Caughey§

NIAID, National Institutes of Health, Rocky Mountain Laboratories, Hamilton, Montana 59840, and Department of Biochemistry, Colorado State University, Ft. Collins, Colorado 80523

Received April 3, 1991; Revised Manuscript Received May 28, 1991

ABSTRACT: A protease-resistant form of the protein PrP (PrP-res) accumulates in tissues of mammals infected with scrapie, Creutzfeldt-Jakob disease, and related transmissible neurodegenerative diseases. This abnormal form of PrP can aggregate into insoluble amyloid-like fibrils and plaques and has been identified as the major component of brain fractions enriched for scrapie infectivity. Using a recently developed technique in Fourier transform infrared spectroscopy which allows protein conformational analysis in aqueous media, we have studied the secondary structure of the proteinase K resistant core of PrP-res (PrP-res 27-30) as it exists in highly infectious fibril preparations. Second-derivative analysis of the infrared spectra has enabled us to quantitate the relative amounts of different secondary structures in the PrP-res aggregates. The analysis indicated that PrP-res 27-30 is predominantly composed of β-sheet (47%), which is consistent with its amyloid-like properties. In addition, significant amounts of turn (31%) and α-helix (17%) were identified, indicating that amyloid-like fibrils need not be exclusively β-sheet. The infrared-based secondary structure compositions were then used as constraints to improve the theoretical localization of the secondary structures within PrP-res 27-30.

Scrapie is a member of a group of neurodegenerative diseases of animals and humans called the transmissible spongiform encephalopathies. One hallmark of these diseases is the presence of abnormal fibrils in extracts of infected brain, as observed initially with scrapie-infected mice (Merz et al., 1981). Subsequent studies have shown that the major protein component of these amyloid-like fibrils is a disease-specific, protease-resistant form of PrP (PrP-res)[1] (Diringer et al., 1983; Prusiner et al., 1983; DeArmond et al., 1985; Merz et al., 1987). Unlike the normal proteinase K sensitive, detergent-soluble PrP (PrP-sen) of both uninfected and infected hosts, PrP-res was identified as the predominant protein of brain fractions enriched for scrapie infectivity (Bolton et al., 1982; Diringer et al., 1983; Gabizon et al., 1988). Because the infectious agents of scrapie and related neurodegenerative diseases are highly resistant to treatments harmful to nucleic acids, it has long been postulated that these agents are devoid of nucleic acid and composed primarily of protein (Alper et al., 1967; Griffith, 1967; Pattison & Jones, 1967; Prusiner, 1982). More recently, it was proposed that PrP-res, or the fibril it forms, is the transmissible agent (Bolton et al., 1982; Diringer et al., 1983; McKinley et al., 1983; Merz et al., 1983). The importance of PrP in these diseases has been underscored by molecular genetic data indicating that variations in the host PrP gene, which encodes both PrP-res and PrP-sen, appear to influence the incubation time (Carlson et al., 1986, 1988; Westaway et al., 1987; Race et al., 1990) and susceptibility to disease (Hsiao et al., 1989; Scott et al., 1989; Doh-ura et al., 1989; Goldgaber et al., 1989). However, it is not yet certain whether PrP-res is the transmissible agent itself, a component of the agent, or a byproduct of the disease which

† This work has been supported in part by grants to W.S.C. from the U.S. Public Health Service (HL-15980) and the Colorado Agricultural Experiment Station (Project 643).
* To whom correspondence should be addressed.
‡ Rocky Mountain Laboratories.
§ Colorado State University.

[1] Abbreviations: PrP-res, proteinase K resistant PrP; Prp-res 27-30, proteinase K digested PrP-res; PrP-sen, proteinase K sensitive PrP; Tris, tris(hydroxymethyl)aminomethane; PBS-S, phosphate-buffered saline with 0.5% sulfobetaine 3-14; SDS, sodium dodecyl sulfate; PAGE, polyacrylamide gel electrophoresis; TBST, Tris-buffered saline with 0.05% Tween 20.

0006-2960/91/0430-7672$02.50/0

coincidently cofractionates with scrapie infectivity.

A number of studies have suggested that the differences between PrP-res and PrP-sen arise at the posttranslational level (Chesebro et al., 1985; Oesch et al., 1985; Basler et al., 1986; Caughey et al., 1988; Borchelt et al., 1990). Strong evidence for this has been obtained recently in scrapie-infected neuroblastoma cells (Caughey & Raymond, 1991). Several posttranslational modifications of PrP are known to occur including the addition of N-linked glycans and a glycophosphatidylinositol moiety (Bolton et al., 1985; Manuelidis et al., 1985; Stahl et al., 1987, 1990a; Caughey et al., 1988, 1989b). However, no scrapie-specific covalent modifications of PrP have been identified. Thus, it is possible that the unusual properties of PrP-res are due to conformational abnormalities.

Little is known about the conformation(s) of PrP other than what has been predicted theortically on the basis of its amino acid sequence (Locht et al., 1986; Bazan et al., 1987; Caughey et al., 1989a). Detailed conformational studies of PrP-res by circular dichroism spectroscopy, nuclear magnetic resonance spectroscopy, and X-ray crystallography are hampered by the insoluble nature of concentrated PrP-res preparations and the unavailability of PrP-res crystals. However, a recently developed technique permits the determination of the relative amounts of different types of secondary structure for proteins in aqueous media by infrared spectroscopy (Dong et al., 1990; Gorga et al., 1989). Since infrared spectroscopy does not require that a molecule be in solution, we have chosen it as the method to analyze the secondary structure of PrP-res aggregates. In the present study, we describe the secondary structure of the protease-resistant core of PrP-res (PrP-res 27–30) as it exists in preparations that contain fibrils and high levels of scrapie infectivity. Our analysis indicates that PrP-res 27–30 is predominantly composed of β-sheet and turns, with a smaller amount of α-helix and very little random-coil structure. This knowledge of the secondary structure composition has allowed us to refine the theoretical localization of the secondary structures within the PrP-res 27–30 molecule.

Materials and Methods

PrP-res 27–30 Purification. Syrian hamsters were inoculated intracerebrally with the 263K strain of scrapie and sacrificed during the clinical phase of disease (usually 70–75-days postinoculation). PrP-res 27–30 was purified from the hamster brains by the procedure of Bolton et al. (1987) except that 1% sulfobetaine 3–14 (Zwittergent 3–14, Calbiochem) was substituted for sarkosyl (*N*-laurylsarkosine) in all solutions but the initial homogenization buffer. The final pellet (P_4) was sonicated (cuphorn probe, Heat Systems Ultrasonics) in 0.2 mL of 10% (w/v) NaCl, 1% (w/v) sulfobetaine 3–14, 1 mM ethylenediaminetetraacetic acid, 1 mM dithiothreitol, and 10 mM Tris-HCl, pH 8.3, per gram of starting brain tissue to obtain a fine suspension. Proteinase K was added to a concentration of 25 μg/mL, and the suspension was incubated 60 min at 37 °C. The digestion was terminated by the addition of phenylmethanesulfonyl fluoride to 1 mM. The PrP-res was pelleted at 184000*g*(max) for 30 min at 20 °C, washed twice with 0.15 M NaCl, 10 mM sodium phosphate, pH 7.2, and 0.5% sulfobetaine 3–14 (PBS-S) at 4 °C, and resuspended by sonication into PBS-S at a concentration of 10 mg/mL. This suspension was designated PrP-res 27–30.

Sodium Dodecyl Sulfate (SDS)–Polyacrylamide Gel Electrophoresis (PAGE) and Immunoblotting. Proteins were separated by SDS–PAGE (12.5% acrylamide) as described (Laemmli, 1970). Silver staining of proteins was performed according to the previously described method (Blum et al., 1987). The intensities of bands in silver-stained gels were compared with an LKB Ultrascan XL laser densitometer. Proteins were electroblotted onto Immobilon P (Millipore, Bedford, MA) using a standard buffer (Towbin et al., 1979) supplemented with 0.01% SDS. The Immobilon P filter was blocked with 5% nonfat dried milk in 10 mM Tris-HCl, pH 8.0, 150 mM NaCl, and 0.05% Tween 20 (TBST). The filter was incubated for 2 h at ambient temperature with a rabbit antiserum (R27) diluted 1:2000 in TBST. Antiserum R27 was raised against a synthetic PrP peptide (1b) coupled to keyhole limpet hemocyanin as described (Wiley et al., 1987). After being washed in TBST, the filter was developed with a kit using alkaline phosphatase conjugated goat anti-rabbit immunoglobulin (Protoblot, Promega, Madison, WI).

Electron Microscopy. PrP-res 27–30 (10 mg/mL) was diluted 1:10 in PBS-S, sonicated, and applied in 2–3-μL aliquots to parlodion-coated, 300-mesh copper electron microscopy grids prepared by the method of Garon (1981). PrP-res 27–30 was allowed to adsorb to the parlodion film for 10 min at ambient temperature. The supernatant was removed and replaced with water for 5 min and then negatively stained with 0.5% ammonium molybdate [$(NH_4)_6Mo_7O_{24}\cdot H_2O$], pH 7, for 30 s. After removal of the excess stain, the grids were air-dried and examined with a Hitachi HU-11E-1 transmission electron microscope at 75 kV.

Scrapie Infectivity Assay. Serial 10-fold dilutions of sonicated PrP-res 27–30 were diluted in phosphate-buffered saline containing 5% fetal bovine serum. Aliquots of 0.05 mL were inoculated intracerebrally into 18–24-day-old Syrian hamsters (six per dilution), and the time to death with clinical scrapie was monitored. Estimates of scrapie infectivity were obtained by comparing average incubation times from appropriate dilutions to a standard curve generated from a purified PrP-res sample of known minimum infectivity according to an end-point dilution assay (Prusiner et al., 1980).

Infrared Spectroscopy. PrP-res 27–30 was sonicated with a cuphorn probe to make a fine suspension immediately before being loaded into an infrared cell with $CaFl_2$ plates and a 6-μm path-length spacer. Spectra were recorded with a Perkin-Elmer Model 1800 FT-IR spectrophotometer at 20 °C. For each spectrum, a 1000-scan interferogram was collected in the single-beam mode with 2 cm^{-1} resolution and a 1 cm^{-1} interval from 4000 to 1000 cm^{-1}. Reference spectra were recorded under identical conditions with only the media in which protein was suspended in the cells. The spectral processing and determination of the relative amounts of different secondary structures from the relative intensities of corresponding bands in the second-derivative amide I spectra were performed as described earlier (Dong et al., 1990). A nine-point smoothing function was applied to the primary spectral data prior to differentiation.

Theoretical Analysis of PrP-res 27–30 Structure. Analyses of the protein secondary structure, hydrophilicity, and residue surface probability were carried out by using previously described algorithms (Garnier et al., 1978; Chou & Fasman, 1977; Emini et al., 1985) with the aid of PC-Gene (Intelligenetics, Mountain View, CA) and Sequence Analysis Package (Genetics Computer Group, Inc., Madison, WI). For these analyses, Convex 330 and IBM PS/2 computers were used. The decision constants employed in the Garnier secondary structure prediction for α-helix, β-sheet, turn, and random coil were 20, −125, −55, and 0, respectively.

Results

Purification of PrP-res 27–30. Initial purifications of

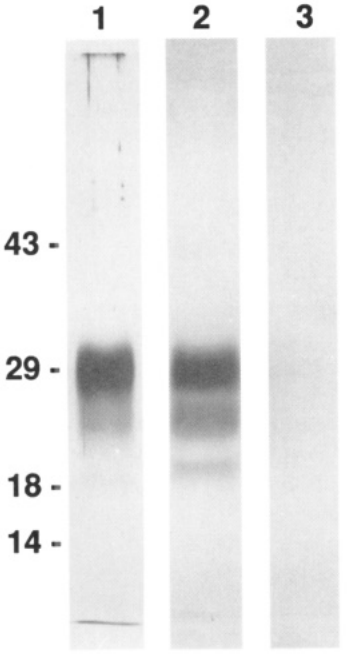

FIGURE 1: SDS–PAGE and immunoblot analyses of PrP-res 27–30. 500 and 50 ng of PrP-res 27–30 preparation B was electrophoresed into lanes of a 12.5% acrylamide SDS–PAGE gel destined for silver staining (lane 1) or immunoblotting (lanes 2 and 3), respectively. The immunoblot filter after lane 2 was reacted with antiserum R27 to identify the PrP bands. The PrP specificity of the R27 reaction was demonstrated by preabsorbing the antiserum with the pure synthetic PrP peptide 1b antigen (lane 3).

PrP-res were performed by using the method of Bolton et al. (1987). However, the strong infrared absorbance (maximum = 1598 cm^{-1}) of the detergent sarkosyl used in the Bolton procedure obscured critical regions of the protein infrared spectrum. To eliminate the effect of sarkosyl in the infrared spectrum, the detergent sulfobetaine 3–14 was substituted for sarkosyl in later steps of the procedure as described under Materials and Methods. Sulfobetaine 3–14 did not interfere with the interpretation of the protein infrared spectrum (data not shown). To improve the homogeneity of the product and reduce the size of the PrP-res aggregates so that they could be loaded into a 6-μm path-length infrared spectroscopy cell, proteinase K treatment was also added. Proteinase K has been shown to remove ~67 amino acids from the N-terminus of hamster PrP-res (already lacking its signal peptide) to yield PrP-res 27–30 without decreasing the scrapie infectivity in the preparations unless excessive concentrations of proteinase K are used for extended periods of time (Prusiner et al., 1984; Hope et al., 1986; McKinley et al., 1983; Neary et al., 1991).

The final proteinase K treated product of this procedure was analyzed by SDS–PAGE followed by silver staining and immunoblotting (Figure 1). Silver staining revealed a major band at M_r = 27 000–30 000 and weaker bands at M_r = 23 000–25 000 and M_r = 19 000 (Figure 1, lane 1). Laser densitometry indicated that these three bands comprised 94% of the silver-stained material in the lane. All three of these bands bound rabbit antisera raised against a synthetic peptide fragment of PrP coupled to keyhole limpit hemocyanin (Figure 1, lane 2). This binding was eliminated by preabsorption of the antiserum with the free PrP peptide antigen, indicating that the molecules within the bands contained the PrP epitope (Figure 1, lane 3). The relative intensities and mobilities of these bands were consistent in three separate preparations analyzed by infrared spectroscopy and agreed well with those reported by others who have purified PrP-res 27–30 using a proteinase K treatment (Bolton et al., 1982, 1985; Diringer et al., 1983; Prusiner et al., 1984). The minor components at M_r = 23 000–25 000 and 19 000 are likely to be less glycosylated forms of PrP-res 27–30 (Hope et al., 1988; Caughey et al., 1989b).

FIGURE 2: Electron microscopic analysis of PrP-res 27–30. Appearance of PrP-res 27–30 aggregates negatively stained with 0.5% ammonium molybdate. Magnification = 78750×. Bar = 100 nm.

Electron Microscopic Analysis of PrP-res 27–30. Since it has been reported previously that purified PrP-res 27–30 can form fibril or rodlike structures (Diringer et al., 1983; Prusiner et al., 1983), we checked the appearance of our PrP-res 27–30 aggregates by negative-stain electron microscopy. Figure 2 shows that our PrP-res 27–30 preparation contained a predominance of clumped rodlike structures. There was no evidence of other macromolecular structures in the preparation. The overall fibrils were generally 10–20 nm in diameter and 50–120 nm in length and contained subfilaments of ~5 nm in width. Some broader, more sheetlike aggregates of up to four subfilaments were also visible. The appearance of these aggregates is similar to those described for other earlier preparations of PrP-res except that the average length of the aggregates in our preparation was slightly shorter than previous reports (Merz et al., 1981, 1987; Diringer et al., 1983; Prusiner et al., 1983). This may be due to the extensive sonication of our PrP-res 27–30 preparations.

Scrapie Infectivity in the PrP-res 27–30 Preparation. To verify that our preparation of PrP-res 27–30 contained high levels of hamster scrapie infectivity, we estimated the infectivity by an incubation time bioassay. The specific infectivity of our preparation was estimated to be at least $10^{11.7}$ LD_{50}/mg of protein, which compared favorably with determinations for PrP-res 27–30 isolated by other methods (Bolton et al., 1987; Gabizon et al., 1988).

Infrared Spectra of PrP-res 27–30. The primary spectrum of PrP-res 27–30 contained major amide I and II bands with maxima at 1636 and 1549 cm^{-1} which was characteristic of protein spectra (Figure 3). When the PrP-res 27–30 spectrum was obtained in D_2O-based medium, the amide II band shifted to a lower wavenumber (max = 1455 cm^{-1}). This D_2O–dependant shift was similar to shifts observed in other proteins (Susi & Byler, 1986) and indicated that most of the exchangeable amide hydrogens were replaced by deuteriums.

Since hamster PrP-res has been shown to contain *N*-acetylglucosamine (Endo et al., 1989), we were concerned that there may be absorptions in the amide I region from the carbohydrate amide groups. Spectra of pure *N*-acetylglucosamine in the H_2O buffer in fact showed a broad band with a maximum at 1638 cm^{-1} (Figure 4). However, since it is known that approximately 12 *N*-acetylglucosamine moieties are present per PrP molecule (Endo et al., 1989), we were able to estimate that the *N*-acetylglucosamine contribution to the amide I region should amount to only about 6% of the total intensity (Figure 4). Digital subtraction of the appropriately factored *N*-acetylglucosamine spectrum from the PrP-res spectrum had little effect on the overall appearance of the spectrum or the conclusions based on subsequent second-derivative analyses (see below). The minimal spectral

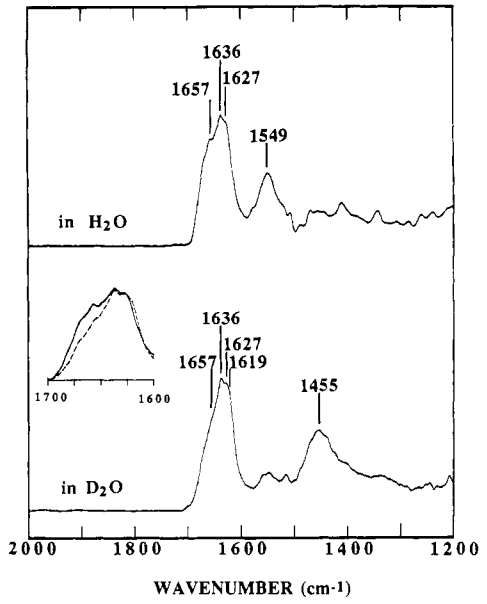

FIGURE 3: Infrared spectra of PrP-res 27–30 in H_2O and D_2O buffers. The contributions of the buffer and water vapor have been subtracted from the primary spectra. The amide I and II regions are the major bands between 1600–1700 and 1500–1600 cm^{-1}, respectively. The inset shows an overlay of the amide I regions of the H_2O (solid line) and D_2O (dashed line) spectra. The sonicated PrP-res 27–30 suspension was at a concentration of 10 mg/mL in PBS-S. The D_2O exchange was performed by washing the PrP-res 27–30 fibrils 3 times in D_2O by centrifugation and sonicating them at 10 mg/mL in the above sulfobetaine buffer prepared with D_2O. The spectrum was collected approximately 16 h after the D_2O washes.

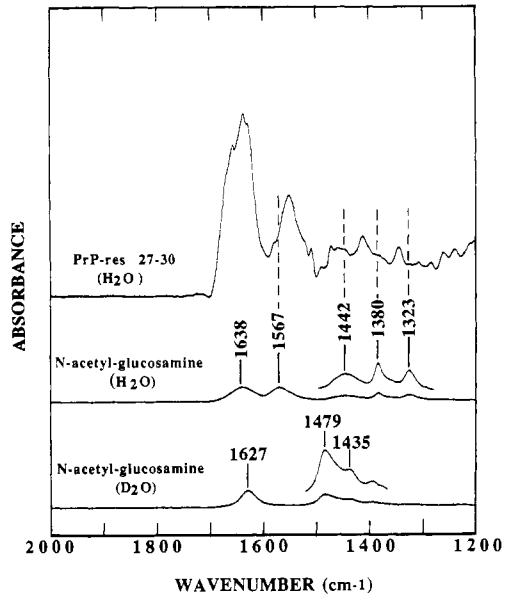

FIGURE 4: Comparison of infrared spectra of PrP-res 27–30 and *N*-acetylglucosamine. The buffer-subtracted and water vapor subtracted *N*-acetylglucosamine spectra were obtained at 50 mM in PBS-S and then were digitally adjusted to approximate the concentration of *N*-acetylglucosamine (7 mM) estimated to be present in 10 mg/mL PrP-res 27–30. To show the positions of the weaker bands in the *N*-acetylglucosamine spectra, vertical expansions of the specific regions are provided.

contribution of *N*-acetylglucosamine was also confirmed by two further facts. First, characteristic *N*-acetylglucosamine bands that lie outside the amide I region (1567, 1380, and 1323 cm^{-1}) were not readily apparent in the PrP-res 27–30 spectrum (Figure 4). Second, the *N*-acetylglucosamine band at 1638 cm^{-1} was found to be shifted to 1627 cm^{-1} in D_2O; however, no major shift of this sort was observed in either the primary spectrum (Figure 3) or the second-derivative spectrum of PrP-res 27–30 (see below).

The side chains of asparagine, glutamine, arginine, and lysine residues can also absorb at specific frequencies in the amide I region of the infrared spectrum. On the basis of the molar integrated intensity of the side chains of the respective free amino acids [A. Dong and W. S. Caughey, unpublished data (Venyaminov & Kalnin, 1990)] and the number of residues per PrP-res 27–30 molecule, these side-chain absorbances were estimated to individually contribute less than 3% of the total integrated amide I intensity to any given region of the amide I spectrum. These contributions were taken into consideration in subsequent quantitative secondary structure analyses.

In both the H_2O- and D_2O-based PBS-S, the maximum amide I absorbance at 1636 cm^{-1} and the shoulder at 1627 cm^{-1} indicated a predominance of β-sheet structures in the PrP-res 27–30 molecule (Miyazawa & Blout, 1961; Glenner et al., 1974; Chirgadze & Nevskaya, 1976a,b; Susi & Byler, 1986; Krimm & Bandekar, 1986). The weaker peak at 1657 cm^{-1} and the shoulder on the high-wavenumber side of this peak suggested the presence of α-helix and turn structures, respectively.

The replacement of deuteriums for rapidly exchangeable amide hydrogens can result in downward shifts in amide I peak frequences (Arrondo et al., 1988; Holloway & Mantsch, 1989). However, comparison of the spectrum of PrP-res 27–30 after a 16-h incubation in D_2O at room temperature indicated that the most intense peaks in the spectrum at 1627, 1636, and 1657 cm^{-1} remained at the same frequency. A possible explanation for this would be that the amide hydrogens of at least portions of the β-sheet and α-helix structures that the bands represent were resistant to exchange with the solvent deuteriums and thus were likely to be in tightly packed structures or interior regions of the fibril. However, the fact that the amide II band experienced an almost complete D_2O-dependent shift argues that most amide hydrogens were exchanged. Another possibility would be simply that the H → D exchange in these structures had little effect on the amide I band frequencies. Other elements of the amide I spectrum were shifted by the H → D exchange as evidenced by the loss of intensity on the high-wavenumber side and the gain of a shoulder on the low-wavenumber side (see inset, Figure 3).

Second-Derivative Analysis of PrP-res 27–30 Infrared Spectra. To further resolve and quantitate the amide I infrared bands corresponding to the secondary structure components of PrP-res 27–30, the second-derivative spectra were calculated for the PrP-res 27–30 in both the H_2O- and D_2O-based media (Figure 5). In the second-derivative spectrum, the peak frequency of an absorbance is identical with the original peak frequency, but the half-bandwidth is reduced by a factor of 2.7. The peak height is proportional to the original peak height and inversely proportional to the square of the original half-bandwidth (Susi & Byler, 1983, 1986). The net result is that the resolution of bands is enhanced and the relative areas determined as illustrated in Figure 5 have been shown empirically to correlate with secondary structure content (Dong et al., 1990). Thus, the peak frequencies of the most intense bands in the second-differential spectra of PrP-res 27–30 (1657, 1636, and 1627 cm^{-1}) can be seen to correspond to much more poorly resolved bands in the primary difference spectra of Figure 3. Figure 5 identifies the bands corresponding to β-sheet, turns, α-helix, and random-coil structures that were assigned in the second-derivative spectrum of PrP-res 27–30 in H_2O-based PBS-S as described previously (Dong et

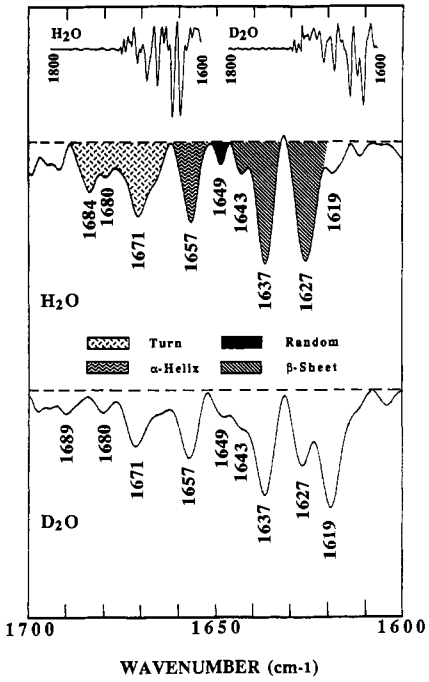

FIGURE 5: Second-derivative infrared spectra (amide I region) of PrP-res 27–30 in H_2O and D_2O. Second-derivative spectra were calculated from the primary difference spectra shown in Figure 3 as described under Materials and Methods. The top two traces are from 1600 to 1800 cm^{-1} to show the spectral base lines above 1700 cm^{-1}. The bottom two traces are expanded views of the amide I regions of the same spectra.

Table I: Secondary Structures of PrP-res 27–30 in Aqueous Suspension As Determined by Amide I Infrared Second-Derivative Analysis[a]

	secondary structure (%)			
preparation	α-helix	β-sheet	turn	random coil
A	15	47	31	7
B	13	50	35	2
C	15	46	35	4
average	14	48	34	4
average (adj)[b]	17	47	31	5

[a] The percentages represent the proportion of the total integrated intensity of the second-derivative amide I spectral bands which corresponds to bands assigned to the designated secondary structure. [b] These averages have been adjusted to eliminate the estimated contributions of *N*-acetylglucosamine and the side chains of asparagine, glutamine, arginine, and lysine to regions of the spectrum assigned to given secondary structures as described in the text.

al., 1990; Gorga et al., 1989).

Previous studies have determined also that the integrated intensities of the bands in the second-differential spectrum in H_2O-based medium are proportional to the amount of the corresponding type of secondary structure in a protein (Dong et al., 1990; Gorga et al., 1989). Application of this type of analysis to spectra from three independent preparations of PrP-res 27–30 in the H_2O buffer confirmed that the predominant types of secondary structure observed were β-sheet and, to a lesser extent, turns (Table I). The α-helix and random-coil contents were more minor components of the secondary structure. When adjustments were calculated to eliminate the estimated maximum contributions of *N*-acetylglucosamine and amino acid residue side chains, there was little effect on the overall secondary structure composition.

Analysis of the second-derivative spectrum of PrP-res 27–30 in D_2O confirmed that much of the PrP-res spectrum was not greatly affected by incubation of the fibrils in D_2O. However,

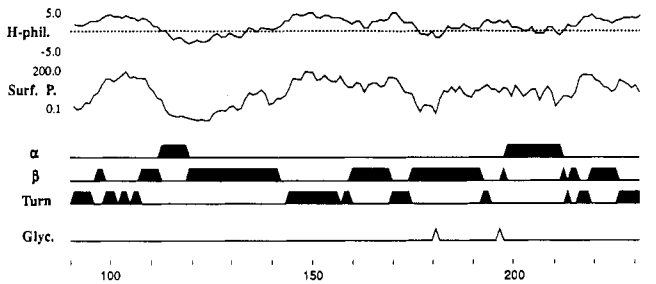

FIGURE 6: PrP-res 27–30 secondary structure predictions by the method of Garnier et al. (1978). The predicted localizations of α-helices (α), β-sheets (β), and turns (Turn) throughout the amino acid sequence of PrP-res 27–30 are shown relative to the hydrophilicity (H-phil.) and log surface probability (Surf. P.) of residues and the potential asparagine-linked glycosylation sites (Glyc.). The numbering and sequence of amino acid residues analysed are based on the full-length cDNA-derived sequence of hamster PrP (Oesch et al., 1985; Robakis et al., 1986). The N- and C-termini of PrP-res 27–30 were those defined by Prusiner et al. (1984) and Stahl et al. (1990a), respectively.

two discrete changes were apparent. In the turn region, the band at 1684 cm^{-1} was shifted to an unknown position (Figure 5). Given that turns are often found near the exterior of molecules, it is not surprising that the amide hydrogens within a turn structure were readily exchanged for deuteriums. However, a significant portion of this effect is likely to be due to the deuterium-dependent shift of peak absorbances from the side chains of asparagine, glutamine, and arginine residues, which, in the spectra of their respective free amino acids at least, shift from maxima of 1680, 1669, and 1673 cm^{-1}, respectively, in H_2O to maxima below 1646 cm^{-1} in D_2O (data not shown). In the β-sheet region, the 1627 cm^{-1} band in the H_2O spectrum was diminished somewhat in intensity relative to the 1637 cm^{-1} band, and a band at 1619 cm^{-1} was intensified. The origin(s) of this band at 1619 cm^{-1} are not clear. Part of it may arise from a solvent-accessible component of the 1627 cm^{-1} β-sheet band in the H_2O spectrum, and part is again attributable to amide side-chain absorptions in D_2O since the infrared spectra of free glutamine and asparagine have an intense band at 1619 and 1622 cm^{-1}, respectively, in D_2O-based phosphate buffer (50 mM, pH 7), whereas absorptions about half as intense are located at 1610 and 1616 cm^{-1}, respectively, in H_2O-based phosphate buffer.

Theoretical Localization of Secondary Structure Components. Having determined the secondary structure composition of PrP-res 27–30 by infrared analysis (Table I), we obtained predictions of the localization of these secondary structures using the algorithm of Garnier et al. (1978). This algorithm has been applied previously to the PrP molecule using only the amino acid sequence (Locht et al., 1986; Bazan et al., 1987; Caughey et al., 1989a). However, the accuracy of such predictions can be improved when the relative amounts of secondary structure components are known (Garnier et al., 1978). Thus, we used the infrared-derived secondary structure compositions in Table I to constrain the Garnier predictions of the major sequence corresponding to PrP-res 27–30 [residues 90–231 of the full-length hamster PrP sequence (Oesch et al., 1985; Stahl et al., 1990a)]. This was done by choosing Garnier decision constants for each individual secondary structure component of PrP-res 27–30 which corresponded to the average of decision constants derived previously for other proteins containing similar amounts of that particular structure (Garnier et al., 1978). Under the constraint of the chosen decision constants, the Garnier method predicted a composition of 14.6% α-helix, 48.2% β-sheet, 30.7% turn, and 6.2% random coil from the PrP-res 27–30 amino acid sequence.

The predicted localization of β-sheet, α-helix, and turn structures is shown in comparison to the PrP hydropathy and surface probability plots in Figure 6. Five strands of β-sheet containing 5–23 amino acid residues were predicted. The 2 longest β-sheet strands and 2 α-helical stretches of 7 and 14 residues were predicted to contain the most hydrophobic and internally disposed regions of the protein. Interestingly, one of the long β-sheet regions contains a potential N-linked glycosylation site (at Asn-181). The addition of a hydrophilic glycan in such a hydrophobic region might have a profound effect on the folding of the PrP molecule. Turns were predicted between β-sheet strands and at the termini in the most hydrophilic and potentially surface-exposed regions.

Discussion

Determination of the Infrared Spectrum of the PrP-res 27–30 Polypeptide Backbone. The analysis of secondary structure from the amide I infrared spectrum requires the accurate determination of the spectrum that is due solely to the peptide linkages in the polypeptide backbone of the protein. Such determinations for proteins in aqueous media in the past have been severely limited by the strong absorbance of both liquid water and water vapor in the amide I region of the spectrum. These water absorbances can now be eliminated satisfactorily from the original spectrum by use of short path-length (6 μm) infrared cells and spectral subtraction techniques (Dong et al., 1990). The study of PrP-res also involves a physical problem due to its tendency to aggregate into particles too large to be readily introduced into cells of such short path length. This problem is especially pronounced with the full-length (nonproteinase K treated) PrP-res and, so far, has prevented our infrared analysis of this PrP form (B. Caughey, A. Dong, and W. S. Caughey, unpublished observations). However, in the case of PrP-res 27–30, sonication immediatley prior to filling the cells was sufficient to allow sample loading. Infrared radiation is of sufficiently long wavelength to eliminate problems with light scattering from the PrP-res 27–30 fibrils, and this gives the infrared method a distinct advantage for the structure determination of such particulate suspensions.

It has become clear that amino acid residue side chains and *N*-acetylglucosamine can absorb in the amide I region of the infrared spectrum and should be considered when quantitative estimates of secondary structure composition are calculated. For the present study, we measured the spectra of separate *N*-acetylglucosamine, asparagine, glutamine, arginine, and lysine in order to estimate their relevant absorbances in the amide I region of the PrP-res 27–30 spectrum. Other investigators have recently reported spectral parameters for the side chains of free amino acids in water which are similar to those we have determined (Venyaminov & Kalnin, 1990). The side-chain spectral parameters may differ somewhat between the free amino acid and the protein microenvironment of an individual residue, but we expect that the average absorbance from all residues of a given amino acid within a protein would be close to that observed for the free amino acid. When summed together, the amino acid side chains and *N*-acetylglucosamine moieties were estimated to contribute ~18% of the integrated intensity in the amide I region of PrP-res 27–30. However, because these contributions were fairly well balanced between the regions assigned to β-sheet and turns, they had only a minor effect on the final secondary structure determination (Table I).

Analysis of PrP-res 27–30 Secondary Structure. Although the primary amide I infrared spectrum indicated a predominance of β-sheet content in PrP-res 27–30, the added resolution of the second-derivative analysis of the spectrum allowed the discrimination of two major β-sheet components with absorbance maxima at 1627 and 1637 cm^{-1}. Possible candidates for such components would be parallel and antiparallel β-sheet. However, we and others have analyzed several proteins with varying amounts of antiparallel and parallel β-sheet according to their X-ray crystal structures and have concluded that the infrared bands arising from these two classes of β-sheet overlap in the 1625–1645 cm^{-1} region and thus are difficult, if not impossible, to discriminate (Susi & Byler, 1987; A. Dong and W. S. Caughey, unpublished experiments). The weak bands observed between 1690 and 1700 cm^{-1} may be cautiously interpreted to indicate the presence of antiparallel β-sheet specifically (Termine et al., 1972; Chirgadze & Nevskaya, 1976a,b; Krimm & Bandekar, 1986; Arrondo et al., 1988; Halverson et al., 1990). It should be noted that antiparallel β-sheet absorbances may also contribute to the region of the spectrum (1663–1689 cm^{-1}) that we have assigned to turns (Miyazawa & Blout, 1961; Susi & Byler, 1986; Halverson et al., 1990). However, in other proteins and polypeptides with β-sheet that is only antiparallel, the β-sheet absorbances are above 1684 cm^{-1} and only approximately one-tenth as intense as the major β-sheet bands in the 1620–1645 cm^{-1} region (Miyazawa & Blout, 1961; Chirgadze & Nevskaya, 1976a,b; Krimm & Bandekar, 1986; Halverson et al., 1990; Arrondo et al., 1988). Thus, we expect that such a β-sheet contribution to the "turn region" absorbance would be minimal. Nonetheless, this consideration suggests that our estimates in Table I of the turn and β-sheet compositions may be slightly high and low, respectively.

The second-derivative infrared analysis of PrP-res 27–30 allowed us to clearly identify other secondary structure components besides the predominant β-sheet structure. The turn composition we have determined for PrP-res 27–30 (31%) is similar to that found in many proteins (Chou & Fasman, 1977; Krimm & Bandekar, 1986) and might be expected to accompany a high antiparallel β-sheet composition. The α-helix content of PrP-res 27–30 was lower than commonly found in globular proteins (Krimm & Bandekar, 1986), and random-coil structures were barely detected. The lack of loosely wound random-coil structures may contribute to the high resistance of PrP-res 27–30 to a variety of proteases.

The effects of partial H → D exchange on the infrared spectrum can shed light on the solvent accessibility of elements of the secondary structure. However, it also complicates the assignment and quantitative interpretation of protein spectra in D_2O since the extent of H → D exchange and the magnitude of its spectral effects are uncertain. Thus, we have been reluctant to attempt the quantitation of secondary structure components from the infrared spectrum of PrP-res 27–30 in the D_2O-based medium.

Refinement of Theoretical Secondary Structure Predictions. Previous theoretical secondary structure analyses of the PrP amino acid sequence have been performed without independent information about secondary structure composition (Locht et al., 1986; Caughey et al., 1989a; Bazan et al., 1987). None of these theoretical treatments predicted that more than about 25% of the PrP-res 27–30 sequence is β-sheet. However, our infrared studies indicated that PrP-res 27–30 has approximately double the initially predicted β-sheet composition and lower than predicted amounts of α-helix and random-coil structures. The major secondary structure compositions determined by the infrared method are expected to be accurate to ±5% based on comparison of infrared-determined protein solution structures with crystal structures (Dong et al., 1990;

Dousseau & Pezolet, 1990). Therefore, our use of the infrared-derived secondary structure compositions to constrain the Garnier analysis of the PrP sequence is likely to have greatly improved the accuracy of the prediction, at least as it relates specifically to the PrP-res 27–30 isoform. These constraints led to the following major changes from the earlier Garnier predictions (Locht et al., 1986; Caughey et al., 1989a): (1) One of the two predicted α-helical domains (the N-terminal one) was shortened. (2) The multiple β-sheet strands that were predicted to be located between the α-helices were fused into three longer β-sheet strands. (3) Additional β-sheet strands were located outside the α-helices (Figure 6). The region previously predicted to be an amphipathic α-helix by Fourier analysis of the primary sequence hydrophobicities (residues 137–157) (Bazan et al., 1987) was assigned turn and β-sheet structures in our Garnier analysis.

The substantial difference between the original unconstrained theoretical predictions and the infrared-based determinations of the secondary structure may be due to the inaccuracy of the former method. Alternatively, it is possible that the unconstrained theoretical methods have accurately predicted the structure of the PrP-sen, but not PrP-res 27–30. This might be the case if the formation of PrP-res involved a major conformational change such as the conversion of regions of the molecule that are normally helical or random coil into β-sheets. Transformations from α-helix to β-sheet have been observed in other amyloidogenic proteins such as insulin (Glenner et al., 1974).

Relationship of Purified PrP-res 27–30 Fibrils to PrP-res in Vivo. Although we have determined the secondary structure composition of PrP-res 27–30 as it exists in detergent-extracted, proteinase K digested amyloid-like fibrils, the question remains as to how this conformation compares to that of PrP-res in live brain tissue. Several considerations suggest that the properties observed for the isolated fibrils are relevant to PrP-res existing in vivo. First is the fact that our preparation is highly infectious, suggesting that, if PrP-res 27–30 is the major component of the scrapie agent, we have done little to alter its viability. However, it must be noted that the accuracy of the bioassay for scrapie infectivity is only good to ± 1 log, so the possibility remains that a majority of the PrP-res 27–30 molecules were in a form that is irrelevant to scrapie infectivity. Second, amyloid-like PrP fibrils have been observed directly in diseased brain tissue, although the fibrils may represent only a small proportion of the total PrP-res in vivo (DeArmond et al., 1985). Like the amyloid-like PrP plaques of diseased brain tissue (Kitamoto et al., 1986), purified PrP-res 27–30 fibrils stained with congo red are birefringent which suggests that both forms have the characteristic β-sheet structure (Prusiner et al., 1983). Finally, the protease resistance exhibited by PrP-res 27–30 also appears to be a characteristic of PrP-res in vivo which is different from PrP-sen (Caughey et al., 1990; Borchelt et al., 1990; Stahl et al., 1990b).

Comparison of PrP-res 27–30 Infrared Spectra with Those of Other Amyloids. The insolubility, protease resistance, fibril formation, and congo red dependent birefringence of PrP-res 27–30 give it properties of an amyloid (Prusiner et al., 1983). Our infrared studies of PrP-res 27–30 are the first of amyloid-like materials in aqueous media. Interestingly, the features of the infrared spectrum of PrP-res 27–30 in the aqueous environment are similar to those of spectra of other types of amyloid fibrils in the dry state or organic solvent systems. For instance, the primary infrared spectra of a variety of natural and synthetic amyloid fibrils in the dry solid state are similar to the aqueous PrP-res 27–30 spectrum in that they have low-wavenumber amide I maxima ($\sim 1632 \pm 3$ cm^{-1}) that are indicative of predominant β-sheet content (Termine et al., 1972; Glenner et al., 1974; Miyazawa & Blout, 1961; Susi & Byler, 1986; Krimm & Bandekar, 1986). The infrared spectrum of highly insoluble fibrils of a synthetic nonapeptide subunit of the Alzheimer's β-protein (β34–42) in 2 M LiBr in tetrahydrofuran with trace D_2O has a single major band at 1625 cm^{-1} which again has been attributed to a β-sheet structure (Halverson et al., 1990) and is similar in wavenumber to one of the two most intense bands in the PrP-res 27–30 spectrum in the H_2O-based medium. It has been suggested that the low wavenumber of such β-sheet bands is indicative of particularly tightly hydrogen bonded β-sheet (Arrondo et al., 1988). The high β-sheet content is consistent with the amyloid-like properties of PrP-res 27–30. However, the second-derivative analysis of the infrared spectrum has enabled us to show clearly that the PrP-res 27–30 fibril is not exclusively β-sheet but also contains significant turn and α-helix components as well.

Applications of Infrared Analysis to the Scrapie Problem. The nature of the difference between the normal PrP-sen and scrapie-associated PrP-res remains a central question in the field of the transmissible spongiform encephalopathies. The results of this study suggest that the infrared techniques applied here to PrP-res 27–30 will allow the direct comparison of the conformations of the normal and scrapie-associated PrP forms and their variants once sufficient quantities of the purified PrP species become available. The enhanced resolution afforded by second-derivative analysis of infrared spectra provides individual conformational "fingerprints" of proteins, e.g., multiple bands in both the turn and β-sheet regions, that can allow more detailed comparisons of conformation than is reflected in the overall secondary structure composition.

Acknowledgments

We thank Drs. Robert Woody, Bruce Chesebro, William Lynch, Michael Robertson, and John Coe for critical review of the manuscript, Dr. John Coligan (NIAID, Bethesda, MD) for synthesizing PrP peptide 1b for us, Ed Schreckendgust for animal care, and Irene Cook Rodriguez for assistance with the manuscript.

References

Alper, T., Cramp, W. A., Haig, D. A., & Clarke, M. C. (1967) *Nature 214*, 764–766.

Arrondo, J. L. R., Young, N. M., & Mantsch, H. H. (1988) *Biochim. Biophys. Acta 952*, 261–268.

Balser, K., Oesch, B., Scott, M., Westaway, D., Walchli, M., Groth, D. F., McKinley, M. P., Prusiner, S. B., & Weissman, C. (1986) *Cell 46*, 417–428.

Bazan, J. F., Fletterick, R. J., McKinley, M. P., & Prusiner, S. B. (1987) *Protein Eng. 1*, 125–135.

Blum, H., Hildburg, B., & Gross, H. J. (1987) *Electrophoresis 8*, 93–99.

Bolton, D. C., McKinley, M. P., & Prusiner, S. B. (1982) *Science 218*, 1309–1311.

Bolton, D. C., Meyer, R. K., & Prusiner, S. B. (1985) *J. Virol. 53*, 596–606.

Bolton, D. C., Bendheim, P. E., Marmostein, A. D., & Potempska, A. (1987) *Arch. Biochem. Biophys. 258*, 579–590.

Borchelt, D. R., Scott, M., Taraboulos, A., Stahl, N., & Prusiner, S. B. (1990) *J. Cell. Biol. 110*, 743–752.

Carlson, G. A., Kingsbury, D. T., Goodman, P. A., Coleman, S., Marshall, S. T., DeArmond, S., Westaway, D., & Prusiner, S. B. (1986) *Cell. 46*, 503–511.

Carlson, G. A., Goodman, P. A., Lovett, M., Taylor, B. A., Marshall, S. T., Peterson-Torchia, M., Westaway, D., & Prusiner, S. B. (1988) *Mol. Cell. Biol. 8*, 5528–5540.

Caughey, B., & Raymond, G. J. (1991) *J. Biol. Chem.* (in press).

Caughey, B., Race, R. E., Vogel, M., Buchmeier, M. J., & Chesebro, B. (1988) *Proc. Natl. Acad. Sci. U.S.A. 85*, 4657–4661.

Caughey, B., Race, R., & Chesebro, B. (1989a) In *Alzheimer's disease and related disorders* (Iqbal, K., Wisniewski, H. M., & Winblad, B., Eds.) pp 619–636, Alan R. Liss, Inc., New York.

Caughey, B., Race, R. E., Ernst, D., Buchmeier, M. J., & Chesebro, B. (1989b) *J. Virol. 63*, 175–181.

Caughey, B., Neary, K., Buller, R., Ernst, D., Perry, L., Chesebro, B., & Race, R. (1990) *J. Virol. 64*, 1093–1101.

Chesebro, B., Race, R., Wehrly, K., Nishio, J., Bloom, M., Lechner, D., Bergstrom, S., Robbins, K., Mayer, L., Keith, J. M., Garon, C., & Haase, A. (1985) *Nature 315*, 331–333.

Chirgadze, Y. N., & Nevskaya, N. A. (1976a) *Biopolymers 15*, 607–625.

Chirgadze, Y. N., & Nevskaya, N. A. (1976b) *Biopolymers 15*, 627–636.

Chou, P. Y., & Fasman, G. D. (1977) *J. Mol. Biol. 115*, 135–175.

DeArmond, S. J., McKinley, M. P., Barry, R. A., Braunfeld, M. B., McColloch, J. R., & Prusiner, S. B. (1985) *Cell 41*, 221–235.

Diringer, H., Gelderblom, H., Hilmert, H., Ozel, M., Edelbluth, C., & Kimberlin, R. H. (1983) *Nature 306*, 476–478.

Doh-ura, K., Tateishi, J., Sasaki, H., Kitamoto, T., & Sakaki, Y. (1989) *Biochem. Biophys. Res. Commun. 163*, 974–979.

Dong, A., Huang, P., & Caughey, W. S. (1990) *Biochemistry 29*, 3303–3308.

Dousseau, F., & Pezolet, M. (1990) *Biochemistry 29*, 8771–8779.

Emini, E. A., Hughes, J. V., Perlow, D. S., & Boger, J. (1985) *J. Virol. 55*, 836–839.

Endo, T., Groth, D., Prusiner, S. B., & Kobata, A. (1989) *Biochemistry 28*, 8380–8388.

Gabizon, R., McKinley, M. P., Groth, D., & Prusiner, S. B. (1988) *Proc. Natl. Acad. Sci. U.S.A. 85*, 6617–6621.

Garnier, J., Osguthorpe, D. J., & Robson, B. (1978) *J. Mol. Biol. 120*, 97–120.

Garon, C. F. (1981) in *Gene Amplification and Analysis* (Chirikjian, J. G., & Papas, T. S., Eds.) Vol. 2, pp 573–585, Elsevier/North-Holland, New York.

Glenner, G. G., Eanes, E. D., Bladen, H. A., Linke, R. P., & Termine, J. D. (1974) *J. Histochem. Cytochem. 22*, 1141–1158.

Goldgaber, D., Goldfarb, L. G., Brown, P., Asher, D. M., Brown, W. T., Lin, S., Teener, J. W., Feinstone, S. M., Rubenstein, R., Kascsak, R. J., & et al. (1989) *Exp. Neurol. 106*, 204–206.

Gorga, J. C., Dong, A., Manning, M. C., Woody, R. W., Caughey, W. S., & Strominger, J. L. (1989) *Proc. Natl. Acad. Sci. U.S.A. 86*, 2321–2325.

Griffith, J. S. (1967) *Nature 215*, 1043–1044.

Halverson, K., Fraser, P. E., Kirschner, D. A., & Lansbury, P. T., Jr. (1990) *Biochemistry 29*, 2639–2644.

Holloway, P. W., & Mantsch, H. H. (1989) *Biochemistry 28*, 931–935.

Hope, J., Morton, L. J. D., Farquhar, C. F., Multhaup, G., Beyreuther, K., & Kimberlin, R. H. (1986) *EMBO J. 5*, 2591–2597.

Hope, J., Multhaup, G., Reekie, L. J. D., Kimberlin, R. H., & Beyreuther, K. (1988) *Eur. J. Biochem. 172*, 271–277.

Hsiao, K., Baker, H. F., Crow, T. J., Poulter, M., Owen, F., Terwilliger, J. D., Westaway, D., Ott, J., & Prusiner, S. B. (1989) *Nature 338*, 342–345.

Kitamoto, T., Tateishi, J., Tashima, T., Takeshita, I., Barry, R. A., DeArmond, S. J., & Prusiner, S. B. (1986) *Ann. Neurol. 20*, 204–208.

Krimm, S., & Bandekar, J. (1986) *Adv. Protein Chem. 38*, 181–364.

Laemmli, U. K. (1970) *Nature 227*, 680–685.

Locht, C., Chesebro, B., Race, R., & Keith, J. M. (1986) *Proc. Natl. Acad. Sci. U.S.A. 83*, 6372–6376.

Manuelidis, L., Valley, S., & Manuelidis, E. E. (1985) *Proc. Natl. Acad. Sci. U.S.A. 82*, 4263–4267.

McKinley, M. P., Bolton, D. C., & Prusiner, S. B. (1983) *Cell 35*, 57–62.

Merz, P. A., Somerville, R. A., Wisniewski, H. M., & Iqbal, K. (1981) *Acta Neuropathol. 54*, 63–74.

Merz, P. A., Somerville, R. A., Wisniewski, H. M., Manuelidis, L., & Manuelidis, E. E. (1983) *Nature 306*, 474–476.

Merz, P. A., Kascsak, R. J., Rubenstein, R., Carp, R. I., & Wisniewski, H. M. (1987) *J. Virol. 61*, 42–49.

Miyazawa, T., & Blout, E. R. (1961) *J. Am. Chem. Soc. 83*, 712–719.

Neary, K., Caughey, B., Ernst, D., Race, R. E., & Chesebro, B. (1991) *J. Virol. 65*, 1031–1034.

Oesch, B., Westaway, D., Walchli, M., McKinley, M. P., Kent, S. B. H., Aebersold, R., Barry, R. A., Tempst, P., Teplow, D. B., Hood, L. E., Prusiner, S. B., & Weissmann, C. (1985) *Cell 40*, 735–746.

Pattison, I. H., & Jones, K. M. (1967) *Vet. Rec. 80*, 2–9.

Prusiner, S. B. (1982) *Science 216*, 136–144.

Prusiner, S. B., Groth, D. F., Cochran, S. P., Masiarz, F. R., McKinley, M. P., & Martinez, H. M. (1980) *Biochemistry 19*, 4883–4891.

Prusiner, S. B., McKinley, M. P., Bowman, K. A., Bendheim, P. E., Bolton, D. C., Groth, D. F., & Glenner, G. G. (1983) *Cell 35*, 349–358.

Prusiner, S. B., Growth, D. F., Bolton, D. C., Kent, S. B., & Hood, L. E. (1984) *Cell 38*, 127–134.

Race, R. E., Graham, K., Ernst, D., Caughey, B., & Chesebro, B. (1990) *J. Gen. Virol. 71*, 493–497.

Robakis, N. K., Sawh, P. R., Wolfe, G. C., Rubenstein, R., Carp, R. I., & Innis, M. A. (1986) *Proc. Natl. Acad. Sci. U.S.A. 83*, 6377–6381.

Scott, M., Foster, D., Mirenda, C., Serban, D., Coufal, F., Walchli, M., Torchia, M., Groth, D., Carlson, G., DeArmond, S. J., Westaway, D., & Prusiner, S. B. (1989) *Cell 59*, 847–857.

Stahl, N., Borchelt, D. R., Hsiao, K., & Prusiner, S. B. (1987) *Cell 51*, 229–240.

Stahl, N., Baldwin, M. A., Burlingame, A. L., & Prusiner, S. B. (1990a) *Biochemistry 29*, 8879–8884.

Stahl, N., Borchelt, D. R., & Prusiner, S. B. (1990b) *Biochemistry 29*, 5405–5412.

Susi, H., & Byler, D. M. (1983) *Biochem. Biophys. Res. Commun. 115*, 391–397.

Susi, H., & Byler, D. M. (1986) *Methods Enzymol. 130*, 290–311.

Susi, H., & Byler, D. M. (1987) *Arch. Biochem. Biophys. 258*, 465–469.

Termine, J. D., Eanes, E. D., Ein, D., & Glenner, G. G. (1972) *Biopolymers 11*, 1103–1113.
Towbin, H., Staehelin, T., & Gordon, J. (1979) *Proc. Natl. Acad. Sci. U.S.A. 76*, 4350–4354.
Venyaminov, S. Y., & Kalnin, N. N. (1990) *Biopolymers 30*, 1243–1257.
Westaway, D., Goodman, P. A., Mirenda, C. A., McKinley, M. P., Carlson, G. A., & Prusiner, S. B. (1987) *Cell 51*, 651–662.
Wiley, C. A., Burrola, P. G., Buchmeier, M. J., Wooddell, M. K., Barry, R. A., Prusiner, S. B., & Lampert, P. W. (1987) *Lab. Invest. 57*, 646–655.

Conformational Studies of a Peptide Corresponding to a Region of the C-Terminus of Ribonuclease A: Implications as a Potential Chain-Folding Initiation Site†

John M. Beals,‡ Elisha Haas,§,‖ Sara Krausz,§ and Harold A. Scheraga*,‡

Baker Laboratory of Chemistry, Cornell University, Ithaca, New York 14853-1301, Department of Life Sciences, Bar-Ilan University, Ramat-Gan, Israel, and Chemical Physics Department, Weizmann Institute of Science, Rehovot, Israel

Received December 26, 1990; Revised Manuscript Received April 5, 1991

ABSTRACT: Conformational properties of the OT-16 peptide, the C-terminal 20 amino acids of RNase A, were examined by nonradiative energy transfer. A modified OT-16 peptide was prepared by solid-phase synthesis with the inclusion of diaminobutyric acid (DABA) at the C-terminus. The OT-16-DABA peptide was labeled with a fluorescent 1,5-dimethylaminonaphthalene sulfonyl (dansyl, DNS) acceptor at the N-terminal amine and a fluorescent naphthoxyacetic acid (NAA) donor at the γ-amine of the DABA located at the C-terminus of the peptide by using an orthogonal protection scheme. Energy transfer was monitored in DNS-OT-16-DABA-NAA by using both fluorescence intensity (sensitized emisson) and lifetime (donor quenching) experiments. The lifetime data indicate that the peptide system is a dynamic, flexible one. A detailed analysis, based on a dynamic model that includes a skewed Gaussian function to model the equilibrium distribution of interprobe distances and a mutual diffusion coefficient between the two probes to model conformational dynamics in the peptide [Beechem & Haas (1989) *Biophys. J. 55*, 1225.], identified the existence of a partially ordered structure (relatively narrow distribution of interprobe distances) at temperatures $\geq$20 °C in the absence of denaturant. The width and the position of the average of the distributions decrease with increasing temperature, in this range; this suggests that the structure is stabilized by hydrophobic interactions. In addition, the peptide undergoes cold denaturation at around 1.5 °C as indicated by broadening of the distance distribution. The addition of 6 M guanidine hydrochloride (Gdn-HCl) also broadens the distance distribution significantly, presumably by eliminating the hydrophobic interactions and unfolding the peptide. The results of the analysis of the distance distribution demonstrate that (1) nonradiative energy transfer can be used to study the conformational dynamics of peptides on the nanosecond time scale, (2) a partially ordered structure of OT-16-DABA exists in solution under typical refolding conditions, and (3) structural constraints (presumably hydrophobic interactions) necessary for the formation of a chain-folding initiation site in RNase A are also present in the OT-16-DABA peptide in the absence of denaturant and are disrupted by Gdn-HCl.

It is generally thought that protein folding is initiated by short-range interactions that result in the formation of one or more chain-folding initiation sites (CFIS)[1] (Matheson & Scheraga, 1978; Wright et al., 1988; Montelione & Scheraga, 1989), formerly termed nucleation sites (Wetlaufer, 1973), within a polypeptide chain. Presumably these CFIS's reduce the amount of conformational space that the whole polypeptide needs to sample prior to folding. One model for identifying CFIS's is based on hydrophobic interactions that induce the formation of short hairpin-like conformations (Matheson & Scheraga, 1978). By computing the free energy of formation of such structures, Matheson and Scheraga (1978) identified several CFIS's in a group of proteins. In particular, several such sites were proposed for the folding of RNase A, the most stable of which was computed to consist of residues 106–118. By using an alternative model, based on the contact map of RNase S, Némethy and Scheraga (1979) identified six CFIS's (designated A–F) and came to similar conclusions about their location within the amino acid sequence.

† This work was supported by grants from the National Institutes of Health (GM-14312) and the National Science Foundation (DMB84-01811). Support was also received from the National Foundation for Cancer Research. J.M.B. was an NIH Postdoctoral Fellow (1987–1990).
* To whom correspondence should be addressed.
‡ Cornell University.
§ Bar-Ilan University.
‖ Weizmann Institute of Science.

[1] Abbreviations: Ac, acetyl; Acm, acetamidomethyl; CFIS, chain-folding initiation site; DABA, diaminobutyric acid; DCC, 1,3-dicyclohexylcarbodiimide; DCM, dichloromethane; DMA, dimethylamine; NHMe, *N*-methylamide; DMF, dimethylformamide; DNS, dansyl; EDTA, ethylenediaminetetraacetic acid; FMOC, *N*-(9-fluorenylmethoxycarbonyl)-; Gdn-HCl, guanidine-HCl; HEPES, 4-(2-hydroxyethyl)-1-piperazineethanesulfonic acid; NAA, naphthoxyacetic acid; NTSB, 2-nitro-5-thiolsulfobenzoate; RNase A, bovine pancreatic ribonuclease A (EC 3.1.4.22); OT-16, the 16th peptide isolated by chromatography from a tryptic (T) digest of oxidized (O) RNase A; D-OT-16, DNS-labeled OT-16-DABA; OT-16-N, OT-16-DABA labeled with NAA; D-OT-16-N, OT-16-DABA labeled with DNS and NAA; D-Lys-N, lysine labeled with DNS and NAA; O-t-Bu, *O-tert*-butyl; t-BOC, *tert*-butoxycarbonyl-; TEAA, triethylammonium acetate; TFA, trifluoroacetic acid; ET, energy transfer; NET, nonradiative energy transfer; NMR, nuclear magnetic resonance; EED, end-to-end distance.

0006-2960/91/0430-7680$02.50/0